Numerical Analysis on Deformation of Braced Excavation with Top-down Method

Y. C. Ding, D. G. Wang, J. C. Liu, K. H. Gu, Z. K. Cheng, and J. H. Wang

Abstract
A three-dimensional simulation based on FLAC3D was carried out to investigate the deformation characteristics of a braced excavation with top-down method in typical Shanghai soft soil deposits. The lateral displacement of the retaining wall, the ground surface settlement, and the subsoil movement outside the excavation were studied in detail. The predicted ground surface settlement curves agree well with the empirical ones, therefore, the reliability of the calculated results is verified, which can provide a useful guidance for engineers in design and analysis of similar excavation projects with top-down method.

Keywords
Numerical simulation • Braced excavation • Top-down method • Deformation • FLAC3D

1 Introduction

Overall stability and safety of retaining structures are the most concerned issues during design and construction of deep excavation of underground basement foundations and other public infrastructures, but in some circumstances especially in heavily congested metropolitan areas, deformation of retaining structures and movement of ground around the excavation should be determined first to appraise the environmental impacts of excavation on the surroundings appropriately (Mana and Clough 1981; Liu et al. 2005).

This paper presents a three-dimensional numerical simulation of a square braced excavation with the top-down construction method in typical Shanghai soft soil deposits based on FLAC3D. The modified Cam-clay constitutive model is used to describe the stress–strain relationship of the soils and the staged excavating as well as the propping processes are dynamically modeled in the numerical model. The lateral displacement of the retaining wall, the ground surface settlement and the ground movement around the excavation are analyzed and discussed.

Y. C. Ding (✉) · D. G. Wang · J. C. Liu · K. H. Gu · Z. K. Cheng
CCCC Third Harbor Consultants Co., Ltd.,
Shanghai 200032, China
e-mail: ycding@163.com

J. H. Wang
Department of Civil Engineering, Shanghai Jiaotong University,
Shanghai 200240, China

2 Numerical Modeling

The braced excavation is square in plan with dimension of 56 × 56 m, and only one quarter of the model is established and modeled regarding the symmetry of the excavation. The maximum excavation depth H_{max} is 20 m, which is divided into five excavation steps with excavation depth of 4 m within each step. The whole dimension of the numerical model is 128 × 128 × 100 m as illustrated in Fig. 1. The strata are modeled with 8-node and 6-face brick elements. The outer cut boundary faces are fixed in normal direction, the central symmetric faces are fixed with symmetric condition, and the base face of the model is fixed in three directions.

The modified Cam-clay constitutive model is employed to describe the deformation behavior of soil, and the variation of groundwater levels is simulated appropriately by

Y. Huang et al. (eds.), *New Frontiers in Engineering Geology and the Environment*,
DOI: 10.1007/978-3-642-31671-5_8,

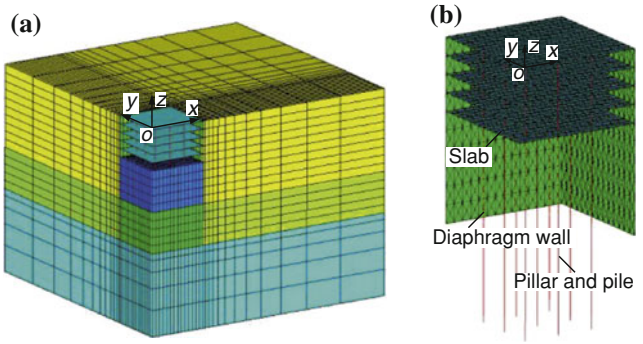

Fig. 1 Mesh of numerical model. **a** Overall model, **b** Retaining structures

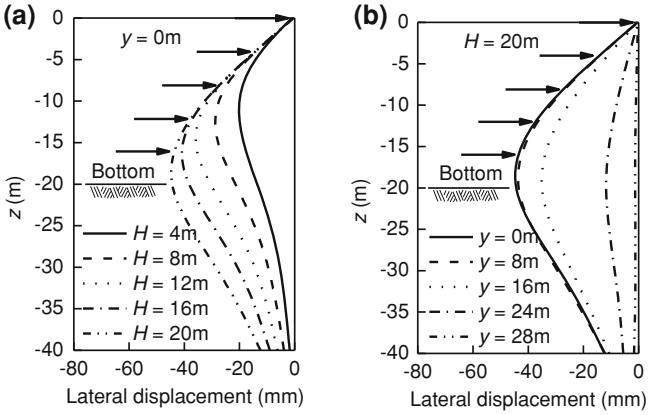

Fig. 2 Lateral displacement of retaining wall

adjusting the location of phreatic surfaces (Potts and Zdravkovic 2001; Wood 1990). The effects of stratification and consolidation are not taken into account in the numerical model, and the property parameters with effective stress conditions are adopted in the analysis. The initial groundwater level is located at 1 m below the ground surface, and the groundwater inside the excavation is drawn to 1 m beneath the excavation bottom during each excavation step. The physical and mechanical parameters of the soils are listed as: the unit weight $\gamma = 17.15\text{kN/m}^3$, the void ratio $e = 1.2$, the lateral at-rest soil pressure coefficient $K_0 = 0.5$, the slope of normal compression line in υ-ln$p$ plan $\lambda = 0.14$, the slope of swelling line in υ-ln$p$ plan $\kappa = 0.01$, the slope of critical state line in p'-q plan $M = 1.2$, the poisson's ratio $\mu = 0.35$ and the overconsolidation ratio $OCR = 1.0$. These property parameters are similar to those for III1 silty clay of Shanghai soft soil deposits.

The horizontal slab struts are modeled with shell elements with equivalent axial stiffness, the retaining walls are modeled with liner elements, and the pillars as well as the piles are modeled with pile elements. The concrete strength grade of C30 is adopted for all retaining walls, struts, pillars and piles, with only 80 percent of strength taken into account regarding the impacts of construction conditions. There are two rows of perpendicular diaphragm walls at $x = 28$ m and $y = 28$ m with depth of 40 m as well as thickness of 1.0 m. There are five levels of horizontal struts with vertical spacing of 4 m and thickness of 0.12 m.

3 Numerical Results and Discussion

3.1 Lateral Displacement of Retaining Wall

The lateral displacement curves of the retaining wall with different excavation depths and at different sections are shown in Fig. 2. The maximum lateral displacement of the retaining wall is −45.3 mm (the negative value indicates that the walls move towards excavation) when the pit is excavated to the bottom. The first level slab strut is installed prior to the excavation of superficial soils within depth of 4 m, resulting in the top of the retaining wall nearly being fixed in horizontal direction during the succeeding excavating processes. The maximum lateral displacements increase gradually with the excavation depth, and the elevations of the maximum lateral displacement points also lower with the excavation depth. The location of the maximum lateral displacement point is near to the excavation bottom face when the pit is excavated to the bottom. The increment of the maximum lateral displacement during each construction stage lowers down with the excavation depth due to the massive axial stiffness of the horizontal slab struts.

There exists a pronounced three-dimensional spatial deformation effect for the retaining wall, with the maximum lateral displacement appearing at the central symmetric section while the minimum value at the corner section, owing to the orthogonal propping effects between the perpendicular diaphragm walls with right-angle intersection.

3.2 Ground Surface Settlement

The ground surface settlement curves with different excavation depths at the symmetric face $y = 0$ m are shown in Fig. 3a. Ground surface upheaval does not appear due to the slipping and the falling-off effects between the retaining wall and the soils modeled with the liner structural elements combined with the interface elements. The maximum upheaval displacement of the retaining wall is 15 mm, while the ground surface settles during all excavation stages. The maximum settlement point occurs near to the excavation boundary when the superficial soils are excavated, then the distance between the maximum settlement

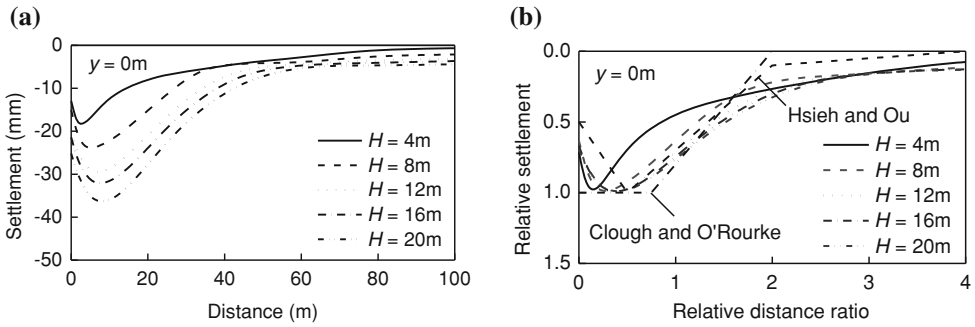

Fig. 3 Ground surface settlement. **a** Absolute settlement, **b** Non-dimensional settlement

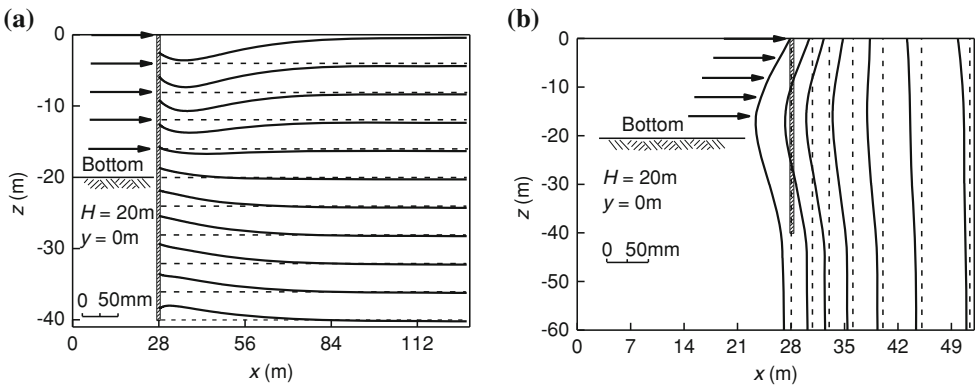

Fig. 4 Soil movement outside excavation. **a** Vertical movement, **b** Horizontal movement

point and the excavation boundary gradually increases with the succeeding excavating. The location of the maximum settlement point almost does not move outward when the excavation depth reaches 12 m.

There also exists a pronounced three-dimensional spatial settlement effect for the ground surface with obvious settlement trough around the middle part of the retaining wall along its longitudinal direction. The maximum ground surface settlement occurs near the central symmetric plane of the excavation with the value of −36.3 mm, while the settlement is much smaller near the corner of the excavation with the value of −16.4 mm. It can be inferred that the settlement of the ground surface and the lateral displacement of the retaining wall are relevant to each other, owing to the same three-dimensional load-bearing and deformation transferring mechanism.

The comparison between the non-dimensional settlement curves of the ground surface versus the relative distance ratio and the empirical envelop curves (Clough and O'Rourke 1990; Hsieh and Ou 1998) is shown in Fig. 3b. The calculated relative settlement curves agree well with the empirical ones, while there are some distinctions when the relative distance ratio is greater than two. The main reasons can be ascribed to: Firstly, the simplified displacement restrictions of the cut boundaries result in the fixed lateral displacement and the free vertical displacement conditions. Secondly, the modified Cam-clay constitutive model can not account for the large stiffness effects when the soils are under small strain state. The more reasonable cut boundary conditions as well as the accurate advanced constitutive models such as Hardening-soil model with Small Strain (HSS model) (Atkinson 2000) are more suitable to predict ground surface settlement characteristic.

3.3 Soil Movement Outside Excavation

The distributions of vertical and horizontal movements of the soils around the retaining wall at the central symmetric plane when the pit is excavated to the bottom are illustrated in Fig. 4. Settlement movements occur for the superficial soils with the maximum settlement points appearing at a short distance to the excavation boundary, while upheaval movements occur for the subsoils with the maximum upheaval points appearing just on the interfaces between the retaining wall and the surrounding soils. The horizontal movements of the ground near the retaining wall are similar to those of the retaining wall, showing a characteristic of deep-level bulge with the maximum lateral displacement adjacent to the excavation bottom face. The elevations of the maximum lateral displacement points for the outer soils

gradually rise with the increase of the distance from the retaining wall, and these points locate at the ground surface eventually.

4 Conclusions

Based on the results of the present study, the following conclusions can be drawn:

(1) The calculated ground surface settlement curves agree well with the published empirical data, indicating the established numerical model can predict the deformation characteristic of the braced excavation with top-down method reasonably and effectively.
(2) The lateral displacement of the retaining wall, the ground surface settlement, and the soil movement around the excavation all interact with each other and combine together to exhibit a pronounced three-dimensional spatial deformation characteristic.
(3) Some calculation conditions are simplified in the numerical model, including simplification of stratification, taking no account of seepage and consolidation due to dewatering. These issues are to be solved in the following studies.

Acknowledgments The research is sponsored by the National Natural Science Foundation of China (No. 50679041) and the Shanghai Leading Academic Discipline Project (No. B208).

References

Atkinson, J. H. (2000). Non-linear soil stiffness in routine design. *Geotechnique, 50*(5), 487–508.

Clough, G. W. & O'Rourke, T. D. (1990). Construction induced movements of in situ walls. In: *ASCE Conference on Design and Performance of Earth Retaining Structures* (pp. 439–470). New York: ASCE.

Hsieh, P. G., & Ou, C. Y. (1998). Shape of ground surface settlement profiles caused by excavation. *Canadian Geotechnical Journal, 35*(6), 1004–1017.

Liu, G. B., Ng, C. W. W., & Wang, Z. W. (2005). Observed performance of a deep multistrutted excavation in Shanghai soft clays. *Journal of Geotechnical and Geoenvironmental Engineering, ASCE, 131*(8), 1004–1013.

Mana, A. I., & Clough, G. W. (1981). Prediction of movements for braced cuts in clay. *Journal of Geotechnical Engineering, ASCE, 107*(6), 759–777.

Potts, D. M., & Zdravkovic, L. (2001). *Finite element analysis in geotechnical engineering: Application*. London: Thomas Telford Ltd.

Wood, D. M. (1990). *Soil behaviour and critical state soil mechanics*. Cambridge: Cambridge University Press.